



3D self-supporting heterostructure NiCo-LDH/ZnO/CC electrode for flexible high-performance supercapacitor



Haotian Xiong^{a,1}, Lianlian Liu^{a,1}, Liang Fang^{a,b,*}, Fang Wu^{a,**}, Shufang Zhang^c, Haijun Luo^{d,**}, Cunzhu Tong^b, Baoshan Hu^e, Miao Zhou^f

^a State Key Laboratory of Power Transmission Equipment & System Safety and New Technology, Chongqing Key Laboratory of Soft Condensed Matter Physics and Smart Materials, College of Physics, Chongqing University, Chongqing 400044, PR China

^b State Key Laboratory of Luminescence and Applications, Changchun Institute of Optics, Fine Mechanics and Physics, Chinese Academy of Sciences, No. 3888 Dong Nanh Road, Changchun, Jilin 130033, PR China

^c College of Software, Chongqing College of Electronic Engineering, Chongqing 401331, PR China

^d Key Laboratory on Optoelectronic Functional Materials, College of Physics and Electronic Engineering, Chongqing Normal University, Chongqing 401331, PR China

^e College of Chemistry and Chemical Engineering, Chongqing University, Chongqing 401331, PR China

^f Key Laboratory of Optoelectronic Technology and Systems of the Education Ministry of China, College of Optoelectronic Engineering, Chongqing University, Chongqing 400044, PR China

ARTICLE INFO

Article history:

Received 15 October 2020

Received in revised form 7 December 2020

Accepted 8 December 2020

Available online 11 December 2020

Keywords:

Self-supported composite

ZnO

NiCo-LDH

Core-shell heterostructure

Flexible supercapacitor

ABSTRACT

Two kinds of nanostructured ZnO, namely nanorods (ZnO NR) and nanoflakes (ZnO NF) were first prepared on conductive flexible carbon cloth (CC) by a hydrothermal route. Then nickel cobalt layered double hydroxide (NiCo-LDH) nanoflakes were directly hydrothermally deposited on them to construct three-dimensional (3D) self-supporting heterostructure NiCo-LDH/ZnO NR/CC and NiCo-LDH/ZnO NF/CC flexible electrodes. The effects of different nanostructured ZnO on morphology, structure and electrochemical performance of NiCo-LDH/ZnO/CC composite materials were investigated. It is found that NiCo-LDH nanoflakes grown on ZnO NF/CC substrate are more compact and uniform than those on ZnO NR/CC substrate. Moreover, NiCo-LDH/ZnO NF/CC electrode presents better electrochemical properties than NiCo-LDH/ZnO NR/CC electrode with 2.6 times higher specific capacitance (1577.6 F g^{-1} at 1 A g^{-1}), 2.2 times better rate capability, and 1.5 time greater cycle stability, which may be attributed to the larger contact area and more redox-active sites provided by the NiCo-LDH NFs grown on ZnO NFs. Furthermore, the as-assembled solid-state flexible NiCo-LDH/ZnO NF//AC (active carbon) asymmetric supercapacitor (ASC) delivers a maximal energy density of 51.39 Wh kg^{-1} (800 W kg^{-1}) with a high operating window of 1.6 V, and exhibits great cyclic stability with 87.3% capacitance retaining after 1000 cycles, which is higher than many reported ASCs. Finally, two packaged ASCs in series successfully lighted a red light-emitting diode (LED, 2.2 V/20 mA), evincing the potentiality of practical application.

© 2020 Elsevier B.V. All rights reserved.

1. Introduction

The rapid development of portable and wearable electronic devices has issued increased demand for flexible, lightweight, eco-friendly and

high-performance energy storage/conversion equipment [1–3], among which the flexible supercapacitor (SC) has drawn considerable attention ascribed to its outstanding mechanical properties, rapid charge-discharge process, high power density and low cost [4–6].

Layered double hydroxide (LDH), due to its novel layered structure, superior capacitance, high redox activity and environmental friendliness, has become a competitive material for SC application [7–9]. Owing to the synergetic actions of both Co and Ni elements which provide various electrochemical active positions by their several oxidized states, NiCo-LDH possesses outstanding capacitive characteristics [10,11]. For instance, the specific capacitance of $\text{Ni}_{0.32}\text{Co}_{0.68}\text{-LDH}$ nanonetwork [12] prepared by a cathodic deposition method was reported to be 1000 F g^{-1} (5 mV s^{-1}), and that of the

* Corresponding author at: State Key Laboratory of Power Transmission Equipment & System Safety and New Technology, Chongqing Key Laboratory of Soft Condensed Matter Physics and Smart Materials, College of Physics, Chongqing University, Chongqing 400044, PR China.

** Corresponding authors.

E-mail addresses: lfang@cqu.edu.cn (L. Fang), wufang@cqu.edu.cn (F. Wu), luohaijun@cqu.edu.cn (H. Luo).

¹ These authors contributed equally to this work and should be considered as co-first authors.

hydrothermally fabricated $\text{Co}_{0.116}\text{Ni}_{0.884}(\text{OH})_2$ [13] reached 1464.7 F g^{-1} (1 A g^{-1}). Nevertheless, the inherent defect of low conductivity in NiCo-LDH hinders its practical application [14].

One strategy to ameliorate the SC properties of NiCo-LDH is to employ highly conductive materials as backbone to support the active materials, so as to shorten the electronic transmission distance [15]. The conductive material, such as graphite, carbon nanotubes, graphene, and Ag nanowires were tried and the SC of the composites were found to be improved [15–18], but the complex and costly preparation processes of them render it worthwhile to search for new facilely-acquired backbone materials.

Due to its high electric conductivity, notable mechanical characteristics, and excellent chemical stability, ZnO has become a potential candidate for the conductive carrier of NiCo-LDH [19]. ZnO was adopted to compound with other oxide materials to improve the SC capability, such as ZnO@MnO_2 [20], ZnO@NiO [21], $\text{ZnO@Co}_3\text{O}_4$ [22], etc., and the core-shell heterostructure composites of ZnO and NiCo-LDH have been also reported. For instance, I. Shakir et al. [23] fabricated the hybrid arrays of NiCo-LDH nanoflakes (NFs) and ZnO nanowires (NWs) on CC substrate by a two-step hydrothermal method, and found that the composite displayed an augmented specific capacitance of 1927 F g^{-1} , nearly 1.8 time as large as that of the bare NiCo-LDH NFs and improved cycling stability and rate performance. The 3D core-shell heterostructure $\text{ZnO@Ni}(\text{OH})_2$ prepared by H. Niu et al. [19] via a combined process of hydrothermal and electrospinning acquired a far higher specific capacitance (2218 F g^{-1} at 2 mV s^{-1}) than that of the pristine $\text{Ni}(\text{OH})_2$ electrode (1604 F g^{-1}). Two binder-free electrodes (ZnO NFs/NiCo-LDH and ZnO NWs/NiCo-LDH) hydrothermally fabricated by N. T. Trang et al. [24] on Au-coated textile fiber substrates manifested outstanding specific capacitance, energy and power densities, and cycling stability. These remarkable electrochemical properties indicate that introducing ZnO to NiCo-LDH can undoubtedly advance the SC performance. Nevertheless, as far as we know, the effects of different nanostructured ZnO on electrochemical properties of NiCo-LDH/ZnO composites and which kind of nanostructure ZnO is the best are still not clear.

Hence, so as to evaluate the influence of ZnO nanostructure on the morphology, structure and electrochemical properties of the NiCo-LDH/ZnO composite, in this paper, two different nanostructured ZnO, namely ZnO nanorods (NRs) and ZnO nanoflakes (NFs), were first prepared on flexible conductive carbon cloth (CC) through hydrothermal route. Then NiCo-LDH NFs were hydrothermally synthesized on ZnO NR/CC and ZnO NF/CC substrates. Besides, a solid-state flexible ASC was fabricated with NiCo-LDH/ZnO NF/CC, activated carbon, and KOH-PVA (polyvinyl alcohol) gel solution as positive electrode, negative electrode, and electrolyte, respectively. The packaged ASC can light a red LED, which signifies that NiCo-LDH/ZnO NF/CC electrode is capable of practical flexible supercapacitor application.

2. Experimental

As illustrated in Fig. 1, 3D self-supporting core-shell heterostructure ZnO/NiCo-LDH/CC flexible composites were synthesized through a two-step process: First, ZnO NFs and ZnO NRs were individually deposited on CCs via hydrothermal method. Then, NiCo-LDH NFs were hydrothermally prepared on ZnO/CC substrates to form flexible composite electrodes. Parameters and procedures were detailed as follows.

2.1. Preparation of ZnO NF/CC and ZnO NR/CC

CCs ($1 \times 2 \text{ cm}^2$, CeTech Co., Ltd) were first rinsed by acetone solution, anhydrous alcohol and ultrapure water for 15 min, respectively, placed in vacuum drying oven at 50°C for 1 h and weighted.

After 15 min of impregnation in crystal seed solution (1.0976 g zinc acetate + 200 mL ethylene glycol monomethyl ether), 10 min of drying in vacuum oven at 50°C for three times, and 1 h of annealing at 400°C in air, the CCs were sealed in autoclaves separately with ZnO NF growth solution (0.2726 g zinc chloride + 0.1201 g urea + 100 mL ultrapure water) or ZnO NR growth solution (0.4390 g zinc acetate + 0.2804 g urotropine + 100 mL ultrapure water + 0.0861 g polyethyleneimine) and heated in a constant temperature of 95°C for 8 h to deposit ZnO NF and ZnO NR. Lastly, after naturally cooled to room temperature and ultrasonicated for 10 min in absolute alcohol and ultrapure water, respectively, the electrodes were dried for 2 h and weighted.

2.2. Preparation of NiCo-LDH/ZnO/CC

The as-prepared ZnO NF/CC and ZnO NR/CC were soaked in a solution comprised of 0.4362 g $\text{Ni}(\text{NO}_3)_2$, 0.4366 g $\text{Co}(\text{NO}_3)_2$, 60 mL methanol, 15 mL deionized water and 1 g cetyltrimethylammonium bromide, sealed in hydrothermal vessel and heated at 180°C for 24 h to prepare NiCo-LDH nanoflakes. Then, after cleaned by anhydrous alcohol and deionized water for 10 min, the electrodes were dried at 50°C for 6 h. The active material loadings of NiCo-LDH/ZnO NF/CC and NiCo-LDH/ZnO NR/CC were approximately 2 ± 0.05 and $1.6 \pm 0.05 \text{ mg/cm}^2$.

2.3. Fabrication of solid-state flexible ASC

2.3.1. Preparation of electrodes

The synthesized NiCo-LDH/ZnO NF/CC was employed as positive electrode, while 8:1:1 mass ratio of activated carbon, acetylene, and polyvinylidene fluoride (PVDF) in ethanol was ultrasonicated for 30 min, uniformly coated on CC, and dried at 100°C for 3 h as negative electrode.

2.3.2. Preparation of gel electrolyte

PVA-KOH solution was used to prepare the solid-state gel electrolyte. First, 80 mL of ultrapure water was constantly heated and stirred by magnetic stirrer, and 8 g of PVA was added when the temperature reached 95°C . After the homogenous dissolution of PVA, 20 mL of 1 M KOH solution was blended with the viscous solution and stirred until the gel-like electrolyte was obtained.

2.3.3. Packaging of ASC

The active material loaded areas of the two electrodes were immersed in the KOH/PVA gel-like solution for 1 h to ensure sufficient permeation. After natural drying in air, about 1 cm^2 of the electrolyte-abundant parts of the two electrodes were overlapped, separated by filter paper in between. The flexible solid-state ASC was fabricated.

2.4. Characterization

X-ray diffraction system (XRD, Bruker D8 Advance $\text{Cu-K}\alpha$) was operated to analyze the crystalline information and chemical components of the composite materials, whereas scanning electron microscope (SEM, JEOL JSM-7800F) was applied to observe the morphologies of the composites.

2.5. Electrochemical measurements

A three-electrode configuration was employed to carry out the electrochemical properties of single electrode in 1.0 M KOH solution, where the fabricated electrodes ($1 \times 1 \text{ cm}^2$), saturated calomel electrode (SCE) and Pt foil were applied as working, reference and counter electrodes, respectively, while a two-electrode system was used to assess the electrochemical performance of the as-assembled

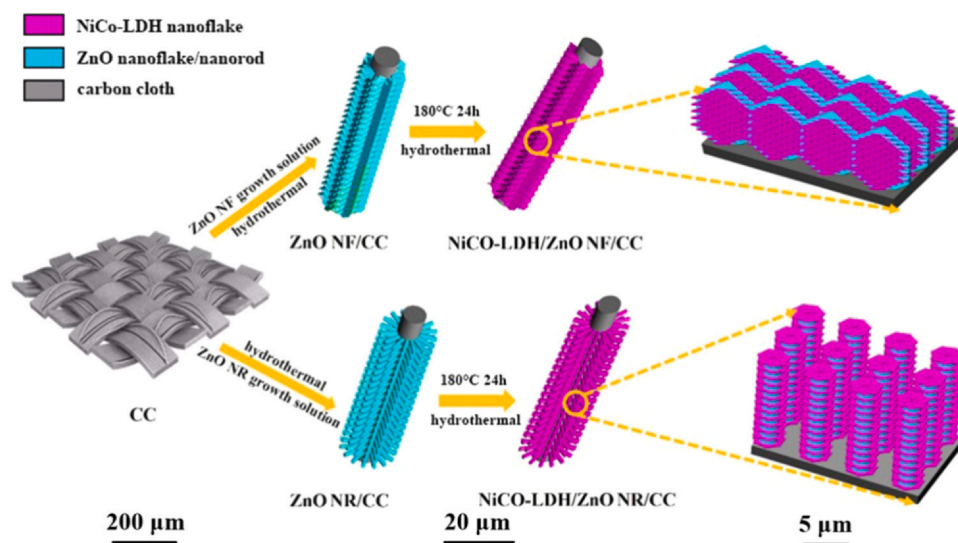


Fig. 1. The synthesis procedure of NiCo-LDH NF on ZnO NF/CC and ZnO NR/CC substrates.

ASC. Galvanostatic charge-discharge (GCD), cycle voltammetry (CV), and electrochemistry impedance spectroscopy (EIS) were tested by electrochemical workstation (CHI760E, Shanghai Chenhua Instrument Company).

The specific capacitance of single electrode can be obtained by the equation as follows:

$$C_s = \frac{I \times \Delta t}{m \times \Delta V} \quad (1)$$

where I and Δt represent the current and time of discharge process, ΔV the operating voltage window, and m the active material mass.

As for fabricated ASC, the specific capacitance, energy density, and power density can be obtained via formulae (2)–(4):

$$C_s = \frac{I \times \Delta t}{m' \times \Delta V'} \quad (2)$$

$$E = \frac{1}{2} \times \frac{1}{3600} \times C_s \times \Delta V^2 \times 1000 \quad (3)$$

$$P = 3600 \times \frac{E}{\Delta t} \quad (4)$$

where $\Delta V'$ and m' correspond to the operating voltage window and the total weight of the two electrodes.

In order to obtain the error of the experiment, three samples of each electrode and ASC were prepared and measured under same condition. The respective standard deviations of the specific capacitance and energy density were given in the corresponding sections of this paper, and the error bars were demonstrated in the corresponding figures.

3. Results and discussion

3.1. Morphology and structure

The XRD patterns of the ZnO, NiCo-LDH/ZnO NF and NiCo-LDH/ZnO NR powders are illustrated in Fig. 2. It displays that the XRD diffraction peaks of both NiCo-LDH/ZnO NF and NiCo-LDH/ZnO NR samples occurred at $2\theta = 12.9^\circ, 24.0^\circ, 34.0^\circ$ and 59.5° , which correlate with the (003), (006), (012) and (110) LDH crystal surfaces respectively, signifying the formation of hydrotalcite-like LDHs (JCPDS No.33-0429), while those at $30.5^\circ, 36.0^\circ, 47.0^\circ$, and 57.1° correspond to the (100), (101), (102), and (110) crystal surfaces of ZnO (JCPDS No.89-1397), implying the successful synthesis of NiCo-LDH/ZnO composites [25].

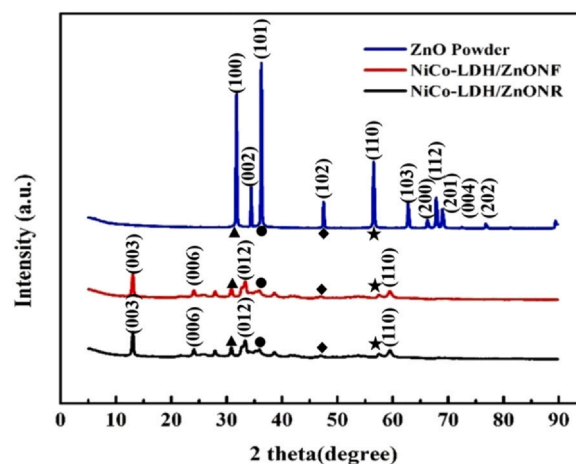


Fig. 2. XRD spectra of ZnO, NiCo-LDH/ZnO NF and NiCo-LDH/ZnO NR samples.

The SEM images of ZnO NR/CC, NiCo-LDH/ZnO NR/CC, ZnO NF/CC and NiCo-LDH/ZnO NF/CC are demonstrated in Fig. 3a–f. Fig. 3a exhibits the rod-like structure of ZnO NR, whereas Fig. 3c shows the petal-like flake structure of ZnO NF. With the deposition of NiCo-LDH NFs, due to the oversized NiCo-LDH NFs, ZnO NR and ZnO NF are completely covered and can scarcely be observed in the SEM images. Meanwhile, as illustrated in Fig. 3c and f, NiCo-LDHs synthesized on ZnO NR/CC substrate (Fig. 3c) are more dispersed and unorganized than those on ZnO NF/CC substrate (Fig. 3f), which possibly results from the reduced crystalline locations caused by the smaller specific surface area of ZnO NR/CC [26].

3.2. Electrochemical properties of NiCo-LDH/ZnO/CC electrodes

Electrochemical behaviors of NiCo-LDH/ZnO NR/CC and NiCo-LDH/ZnO NF/CC were investigated to understand the participation of NiCo-LDH and ZnO in composite electrodes. As shown in Fig. 4a, CV profiles of NiCo-LDH/ZnO NR/CC and NiCo-LDH/ZnO NF/CC manifest two apparent pairs of redox peaks at 5 mV s^{-1} in the voltage range of 0–0.65 V, and the oxidation and reduction peaks can be identified at around 0.35 V and 0.15 V, respectively.

Additionally, according to the literature [27], the redox peak potentials vs. SCE of $\text{Ni}(\text{OH})_2$ are 0.49 V and 0.36 V while those of $\text{Co}(\text{OH})_2$ are respectively 0.57 V and 0.47 V, so the capacitive properties

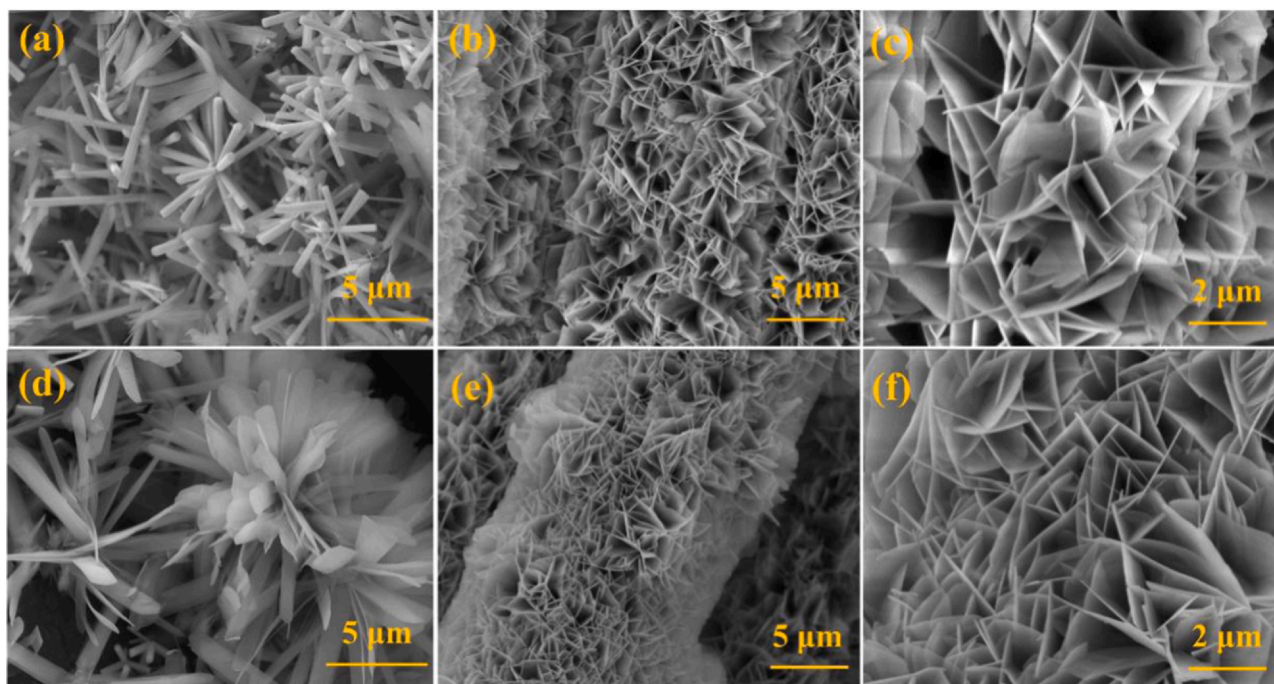


Fig. 3. SEM images of (a) ZnO NR/CC, (b-c) NiCo-LDH/ZnO NR/CC, (d) ZnO NF/CC, and (e-f) NiCo-LDH/ZnO NF/CC.

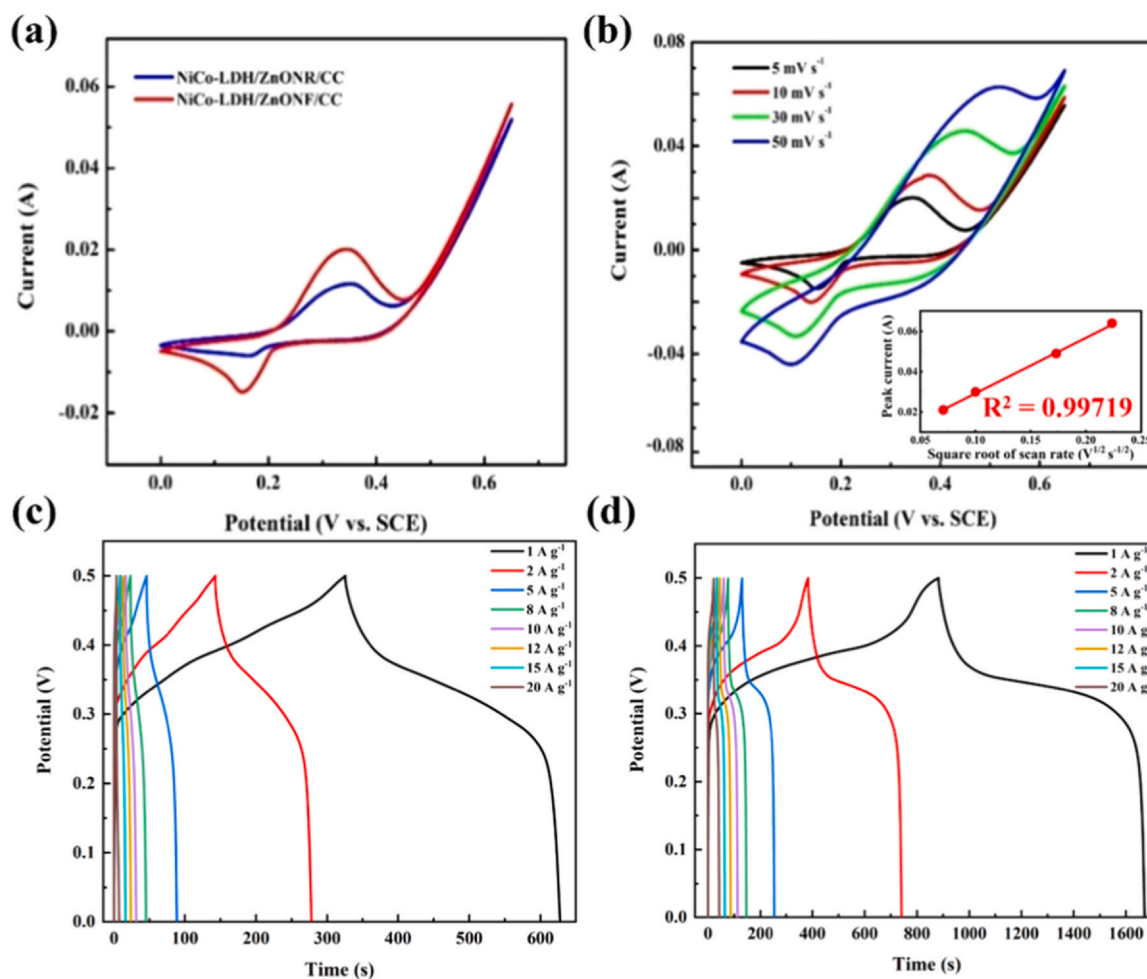
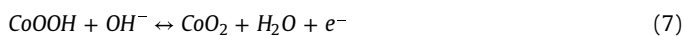
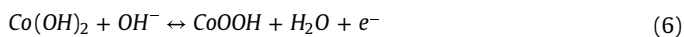
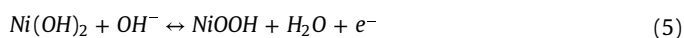


Fig. 4. CV profiles of (a) NiCo-LDH/ZnO NR/CC and NiCo-LDH/ZnO NF/CC electrodes at the scanning speed of 5 mV s⁻¹, and (b) NiCo-LDH/ZnO NF/CC electrode at various scanning speeds. (Inset: the square root of scan rate as a function of the peak discharge current) GCD profiles at various current densities of (c) NiCo-LDH/ZnO NR/CC, and (d) NiCo-LDH/ZnO NF/CC electrodes.

are jointly contributed and primarily dominated by the faradic reactions of Ni^{2+} and Co^{2+} . Chemical reaction equations corresponding to the redox peaks are listed below [28]:



Noteworthy, as manifested in Fig. 4a, the redox peak currents and the integral area of the CV curve of NiCo-LDH/ZnO NF/CC are both larger than those of NiCo-LDH/ZnO NR/CC, which reflects the better capacitance capability of NiCo-LDH/ZnO NF/CC electrode. To further investigate the electrochemical performance of NiCo-LDH/ZnO NF/CC electrode, the CV behaviors at different scan speeds ($5, 10, 30, 50 \text{ mV s}^{-1}$) were researched. In Fig. 4b, the redox peaks can be evidently spotted in every CV curve, meaning that the charge storage and release principally result from the reversible faradic reaction. As the scanning rate increases ($5\text{--}50 \text{ mV s}^{-1}$), the curve configurations almost stay unaltered, suggesting the fast transmission of ions and electrons over the electrode/electrolyte interface; moreover, current increases in pace with the sweep rate, which reveals that the composite electrode is capable of undergoing heavy-current charge and discharge. As shown in the inset of Fig. 4b, the discharge peak currents (i_p , A) are well proportional to the square root of scan rates (v , mV s^{-1}) ($i_p=0.277v^{1/2}$), implying that the electrode reaction of our samples is a diffusion-controlled process.

Fig. 4c demonstrates the different GCD curves of NiCo-LDH/ZnO NR/CC electrode, based on which the specific capacitances calculated via Eq. (1) are 604.2, 540, 428, 347.2, 288, 261.6, 222, and 148 F g^{-1} at 1, 2, 5, 8, 10, 12, 15, and 20 A g^{-1} , respectively, with an average standard deviation of 28.5 F g^{-1} . Likewise, on the basis of Fig. 4d, the specific capacitances of NiCo-LDH/ZnO NF/CC are 1577.6, 1428, 1242, 1116.8, 1060, 991.2, 912, and 856 F g^{-1} (1, 2, 5, 8, 10, 12, 15, and 20 A g^{-1}), with an average standard deviation of 47.6 F g^{-1} .

The relationship of the specific capacitance with current density of NiCo-LDH/ZnO NR/CC and NiCo-LDH/ZnO NF/CC was compared, and the results were plotted in Fig. 5a. As exhibited in Fig. 5a, the specific capacitance of NiCo-LDH/ZnO NF/CC at 20 A g^{-1} is 5.8-fold as large as that of NiCo-LDH/ZnO NR/CC (2.6-fold at 1 A g^{-1}), indicating the marvelous capacitive properties of NiCo-LDH/ZnO NF/CC. In addition, as illustrated in Fig. 5b, the capacitance retention of NiCo-LDH/ZnO NF/CC reaches 89.7% after 5000 continuous cycles at 20 A g^{-1} , which is much better than the 59.4% of NiCo-LDH/ZnO NR/CC. The NiCo-LDH/ZnO NF/CC electrode manifests greater capacitive and cyclic properties probably because the ZnO nanoflakes can be regarded to be composed of many ZnO nanorods, but possess less contact resistance and more stability.

EIS analyses were conducted with the range of frequency varied from 0.01 Hz to 100 kHz. As demonstrated in Fig. 5c, in the high frequency area, the Nyquist semicircle diameter of NiCo-LDH/ZnO NF/CC is shorter than that of NiCo-LDH/ZnO NR/CC, which signifies the lower charge transfer resistance (4.3 Ohm) and better capacitance performance of NiCo-LDH/ZnO NF/CC [29].

The properties of NiCo-LDH/ZnO NF/CC electrode in this work were compared with some previously reported ZnO-based or NiCo-LDH-based electrodes and the results were tabulated in Table 1. As illustrated in Table 1, the specific capacitance of our synthesized electrode (1577.6 F g^{-1} at 1 A g^{-1}) is higher than that of other ZnO-based electrodes, like porous ZnO-NiO (1066.4 F g^{-1} at 5 mV s^{-1}) [21] and ZnO@Co₃O₄ (857.7 F g^{-1} at 1 A g^{-1}) [22], and is comparable to that of ZnO NFs/NiCo-LDH (1624 F g^{-1} at 10 A g^{-1}) [24] and NiCo-LDH/ZnO NWs (1927 F g^{-1} at 2 A g^{-1}) [23], attributed to the numerous electroactive locations afforded by multiple oxidation states in the introduced NiCo-LDH. As for NiCo-LDH-based electrode materials, our fabricated electrode performs better than the majority of them, such as Ni_{0.32}Co_{0.68}-LDH nanonetwork (1000 F g^{-1} at 5 mV s^{-1}) [12], Co_{0.116}Ni_{0.884}(OH)₂ (1464.7 F g^{-1} at 1 A g^{-1}) [13], NiCo-LDH/CNTs (1151 F g^{-1} at 1 A g^{-1}) [32], NiCo-LDH@Au-CuO (1273 F g^{-1} at 7.96 mA cm^{-2}) [33], NiCo-LDH/MXene (983.6 F g^{-1} at 2 A g^{-1}) [34], and NiCo-LDH/NiCo₂O₄ microspheres (1132 F g^{-1} at 2 mA cm^{-2}) [35], ascribed to the increased electron transmission channels provided by the introduced ZnO. Besides, in terms of cycle stability, our prepared NiCo-LDH/ZnO NF/CC electrode are more or comparably stable than most of the reported ZnO-based and NiCo-LDH-based electrodes, namely NiCo-LDH nanosheets (89.5% after 2000 cycles) [11], NiCo-LDH/rGO (74% after 1000 cycles) [16], Co_{0.5}Ni_{0.5}(OH)₂/graphene/CNTs (75% after 5000 cycles) [18], NiCo-LDH/Ag nanowires (89.8% after 2000 cycles) [30], NiCo-LDH/MXene (76% after 5000 cycles) [34], and NiCo-LDH/NiCo₂O₄ microspheres (90% after 2000 cycles) [35], due to ZnO nanoflakes being firm backbones of NiCo-LDH nanoflakes that stabilize the composite. Despite that the specific capacitance of our prepared electrode is slightly smaller than several electrodes on NF (nickel foam) substrate, like NiCo-LDH/rGO (1911.14 F g^{-1} at 2 A g^{-1}) [16] and ZnO@Ni(OH)₂ (2218 F g^{-1} at 2 mV s^{-1}) [19], the employment of CC substrate provides the ability to apply in flexible supercapacitors, broadening the application domains of the electrode and offering more prospects for portable and wearable devices appliance.

3.3. Electrochemical properties of the NiCo-LDH/ZnO NF//AC ASC

So as to evaluate the application potentiality of NiCo-LDH/ZnO NF/CC electrode, solid-state flexible ASCs were constructed with PVA/KOH, NiCo-LDH/ZnO NF/CC, active carbon, and filter paper as

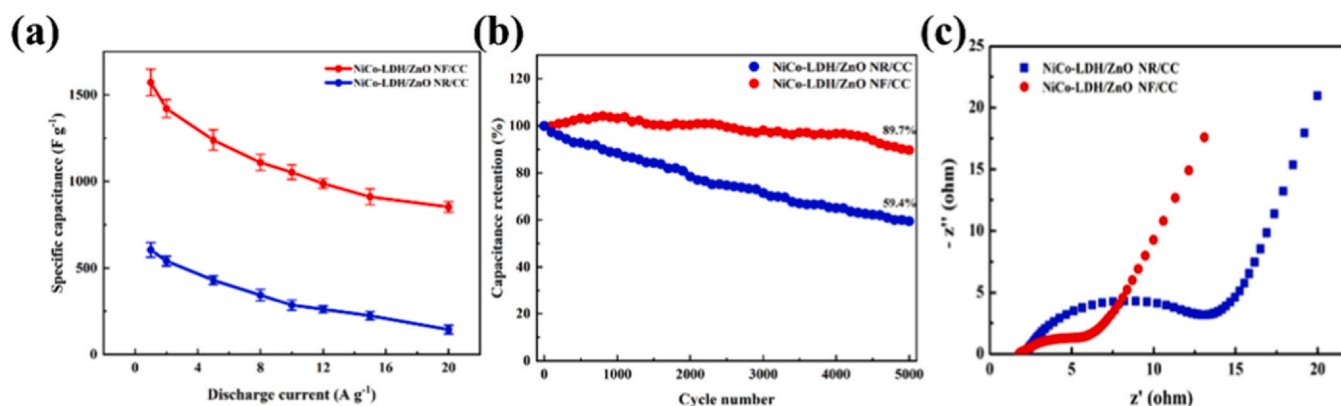


Fig. 5. (a) The trend of specific capacitance values with the increase of discharge current, (b) cycle performance at 20 A g^{-1} , and (c) Nyquist diagram of NiCo-LDH/ZnO NR/CC and NiCo-LDH/ZnO NF/CC electrodes.

Table 1

Electrochemical property comparison of our as-synthesized NiCo-LDH/ZnO NF/CC with ZnO-based or NiCo-LDH-based electrodes in some published papers.

Sample	Substrate ^a	Synthesis method ^a	Electrolyte	C _s (F g ⁻¹)	Cycling stability	Ref.
NiCo-LDH nanosheets	conductive textile	ED	1 M KOH	2105 at 2 A g ⁻¹	89.5% (2000 cycles)	[11]
Ni _{0.32} Co _{0.68} -LDH nanonetwork	NF	cathodic deposition	1 M NaOH	1000 at 5 mV s ⁻¹	100% (1000 cycles)	[12]
NiCo-LDH/rGO	NF	ST	3 M KOH	1911.14 at 2 A g ⁻¹	74% (1000 cycles)	[16]
ZnO@Ni(OH) ₂	NF	electrospinning & HT	6 M KOH	2218 at 2 mV s ⁻¹	100% (1000 cycles)	[19]
porous ZnO-NiO	nickel grid	chemical precipitation	3 M KOH	1066.4 at 5 mV s ⁻¹	99.5% (400)	[21]
ZnO@Co ₃ O ₄ heterostructures	NF	HT	2 M KOH	857.7 at 1 A g ⁻¹	128.7% (6000)	[22]
NiCo-LDH/ ZnO nanowires	CFC	HT	6 M KOH	1927 at 2 A g ⁻¹	96% (3000)	[23]
ZnO nanoflakes/ NiCo-LDH	Au-coated textile fiber	HT	1 M LiOH	1624 at 10 A g ⁻¹	94% (2000)	[24]
NiCo-LDH/CNTs	NF	chemical bath deposition	2 M KOH	1151 at 1 A g ⁻¹	77% (10000)	[32]
NiCo-LDH@ Au-CuO	Cu fiber	in-situ corrosion growth	3 M KOH	1273 at 7.96 mA cm ⁻²	90.8% (30000)	[33]
NiCo-LDH/MXene	NF	ED	6 M KOH	983.6 at 2 A g ⁻¹	76% (5000)	[34]
NiCo-LDH/NiCo ₂ O ₄ microspheres	NF	HT & ED	2 M KOH	1132 at 2 mA cm ⁻²	90% (2000)	[35]
NiCo-LDH/ZnO nanoflakes	CC	HT	1 M KOH	1577.6 at 1 A g ⁻¹	89.7% (3000)	this work

^a ED: electrochemical deposition; NF: nickel foam; HT: hydrothermal; CFC: carbon fiber cloth; ST: solvothermal; CVD: chemical vapor deposition; CC: carbon cloth.

gel electrolyte, positive electrode, negative electrode, and separator, respectively. The CV properties of the two electrodes at a scanning speed of 50 mV s⁻¹ were compared in Fig. 6a. The CV curve of the negative electrode is rectangle-shaped, suggesting its electric double-layer capacitive character, while the apparent redox peaks in the CV configuration of the positive electrode indicate its pseudocapacitive quality. Fig. 6b shows the CV profiles of NiCo-LDH/ZnO NF//AC at various sweep speeds (5–50 mV s⁻¹). All of the curves in Fig. 6b show quasi-rectangular configuration, which denotes the synergic contribution of EDLC and pseudocapacitance at an operating window of 0–1.6 V. In addition, the curves present no distinct deformation as the scanning rate changes, which implies the brilliant charge/discharge ability and rate capacity. Moreover, the GCD

behaviors of the ASC at various current densities (1–8 A g⁻¹) were displayed in Fig. 6c. The charge/discharge processes of the device demonstrate good symmetrical characteristic, reflecting the excellent electrochemical reversibility. By means of bending test, flexibility of the packaged ASC was studied. As exhibited in Fig. 6d, the GCD and CV curves of the device after bending scarcely distorted in comparison to those of the flat state, which suggests the outstanding flexibility of the as-fabricated ASC by virtue of CC substrate, broadening the applicative outlook for wearable and portable devices.

As shown in Fig. 7a, the specific capacitance values of NiCo-LDH/ZnO NF//AC calculated based on formula (2) are 144.5, 115.8, 95.5, 81.1, 71.7, 58.9, 50.5, and 40.8 F g⁻¹ at 1–8 A g⁻¹, respectively, with an

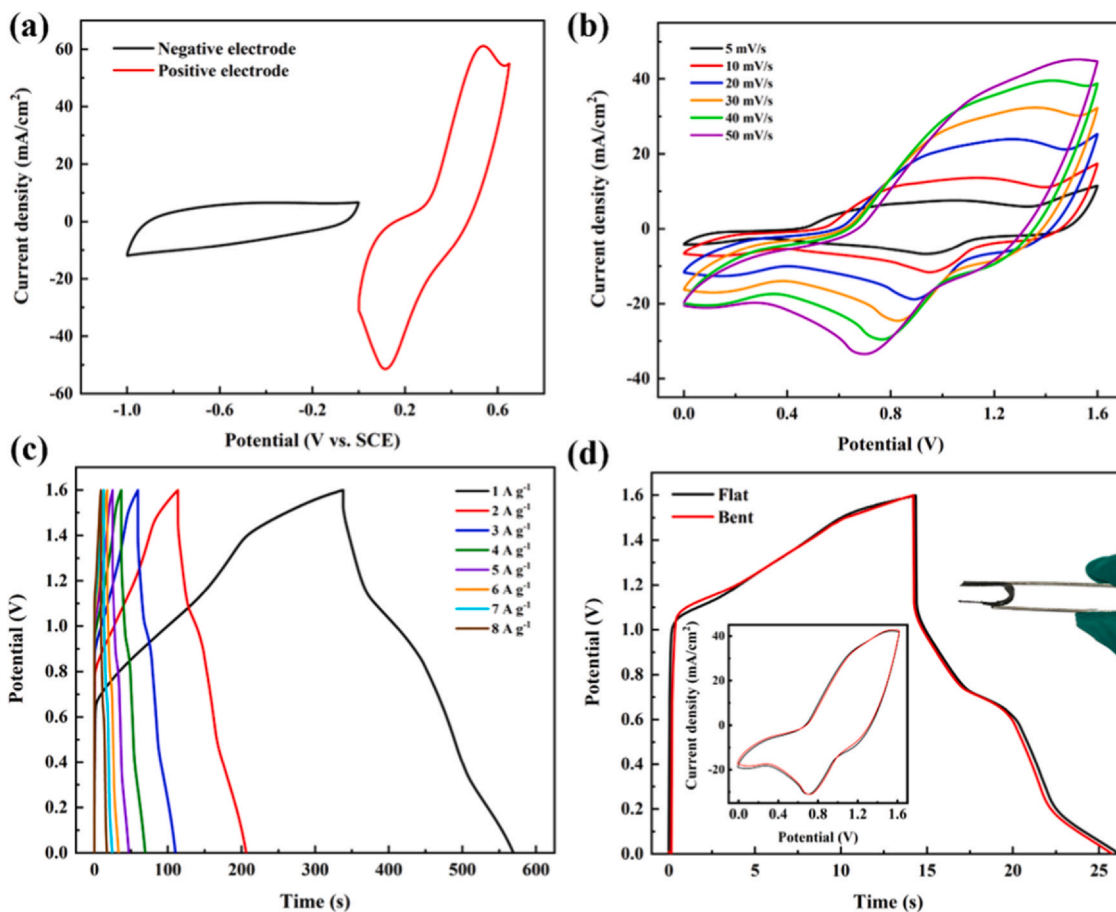


Fig. 6. (a) CV behaviors of negative and positive electrodes at 50 mV s⁻¹. (b) CV and (c) GCD profiles at different conditions of the assembled ASC. (d) GCD curves at 7 A g⁻¹ of the assembled ASC in the flat and bent conditions with insets of CV curves before and after bending at 50 mV s⁻¹ and the photograph of the bent ASC.

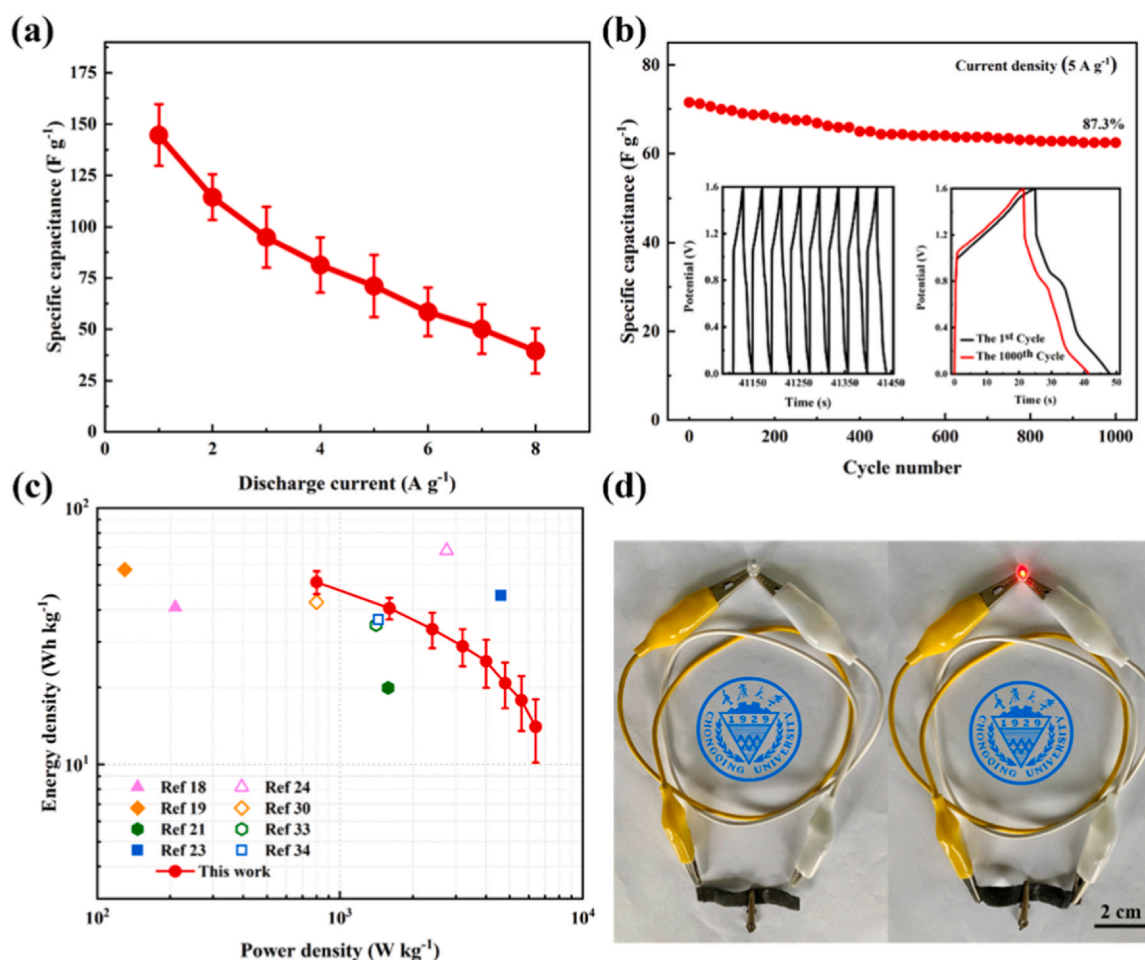


Fig. 7. (a) The trend of specific capacitance values of NiCo-LDH/ZnO NF//AC with the increase of discharge current. (b) cycle performance of NiCo-LDH/ZnO NF//AC at 5 A g⁻¹ with insets of GCD profiles of the 1st and 1000th, and the last eight cycles. (c) Ragone plot. (d) photographs of a red LED powered by two ASCs in series. (For interpretation of the references to colour in this figure legend, the reader is referred to the web version of this article.)

Table 2

Energy density comparison of our as-fabricated NiCo-LDH/ZnO NF//AC with ZnO-based or NiCo-LDH-based ASCs in some published papers.

Positive electrode	Negative electrode	Energy density (Wh kg ⁻¹)	Ref.
Co _{0.5} Ni _{0.5} (OH) ₂ /graphene/CNTs	AC/CNT	41 Wh kg ⁻¹ at 210 W kg ⁻¹	[18]
ZnO@Ni(OH) ₂	carbon fibers	57.6 Wh kg ⁻¹ at 129.7 W kg ⁻¹	[19]
ZnO nanoflakes/NiCo-LDH	AC	68.23 Wh kg ⁻¹ at 2750 W kg ⁻¹	[24]
NiCo-LDH/Ag nanowires	AC	42.9 Wh kg ⁻¹ at 800 W kg ⁻¹	[30]
NiCo-LDH/graphene films	AC	50.2 Wh kg ⁻¹ at 800 W kg ⁻¹	[31]
NiCo-LDH@Au-CuO	carbon fibers	34.97 Wh kg ⁻¹ at 1410 W kg ⁻¹	[33]
NiCo-LDH/MXene	CNT	36.70 Wh kg ⁻¹ at 1440 W kg ⁻¹	[34]
NiCo-LDH/ZnO nanoflakes	AC	51.39 Wh kg ⁻¹ at 800 W kg ⁻¹	this work

average standard deviation of 13 F g⁻¹. Additionally, 1000 continuous cycles of GCD measurement were conducted at 5 A g⁻¹ to assess the cyclic performance of the packaged ASC. As demonstrated in Fig. 7b and the two insets, 87.3% of the capacitance retains after the test, the GCD curves of the 1st and 1000th loops are almost in the same shape, and the curves of last 8 cycles keep consistent, manifesting the impressive cycle stability of the device. Besides, Ragone plot that mirrors the comprehensive performance concerning the energy and power densities was diagrammed in Fig. 7c to contrast our fabricated NiCo-LDH/ZnO NF//AC with some previously reported NiCo-LDH or ZnO based ASCs, and the results were listed in Table 2. As exhibited in Fig. 7c, the energy densities can be calculated to be 51.39, 41.18, 33.97, 28.84, 24.72, 20.93, 17.89, 14.49 Wh kg⁻¹ on the basis of Eqs. (3) and (4) at the power densities of 800, 1600, 2400, 3200, 4000, 4800, 5600, and 6400 W kg⁻¹, respectively, with an average

standard deviation of 4.7 Wh kg⁻¹. The narrow error ranges of our synthesized electrode and assembled ASC device indicate the excellent experiment repeatability and quality uniformity of our samples. The maximal energy density of our fabricated ASC reaches 51.39 Wh kg⁻¹ (800 W kg⁻¹), which is higher than that of many other ASCs demonstrated in Table 2, like NiCo-LDH/graphene/CNTs//AC/CNTs [18] (41 Wh kg⁻¹ at 210 W kg⁻¹), ZnO@Ni(OH)₂//PCNF [19] (57.6 Wh kg⁻¹ at 129.7 W kg⁻¹), NiCo-LDH/Ag/NF//AC [30] (42.9 Wh kg⁻¹ at 800 W kg⁻¹), NiCo-LDH/GF/NF//AC [31] (50.2 Wh kg⁻¹ at 800 W kg⁻¹), CCCH@NiCo-LDH@Au-CuO/Cu//carbon fibers [33] (34.97 Wh kg⁻¹ at 1410 W kg⁻¹), and NiCo-LDH/MXene//CNT [34] (36.70 Wh kg⁻¹ at 1440 W kg⁻¹). Furthermore, as shown in Fig. 6d, two as-fabricated ASCs in series can drive a red LED (2.2 V, 20 mA) after being charged for one minute, revealing their prospects for practical application.

4. Conclusion

In summary, two 3D self-supported flexible electrodes NiCo-LDH/ZnO NR/CC and NiCo-LDH/ZnO NF/CC were successfully synthesized by a two-step hydrothermal route. Our research shows that NiCo-LDH nanoflakes grown on ZnO NF/CC substrate are more compact and uniform than those on ZnO NR/CC substrate, indicating that the ZnO NF/CC substrate will offer a larger specific surface area and more crystalline positions for NiCo-LDH nanoflakes to grow on, which will cause the better electrochemical performance of NiCo-LDH/ZnO NF/CC electrode. Typically, the NiCo-LDH/ZnO NF/CC electrode has an excellent capacitive property (1577.6 F g^{-1} at 1 A g^{-1}), great rate capacity (54.3% capacitance retention at 20 A g^{-1}), and remarkable cycling performance (89.7% capacitance retention after 5000 cycles at 20 A g^{-1}), compared to 604.2 F g^{-1} , 24.5%, and 59.4% of NiCo-LDH/ZnO NR/CC electrode. Furthermore, the as-fabricated NiCo-LDH/ZnO NF//AC ASC attains a considerable energy density of 51.39 Wh kg^{-1} (800 W kg^{-1}), which is higher than many previous reported ASCs, and two ASCs in series can successfully light a red LED (2.2 V, 20 mA) after charged for one minute, indicating that NiCo-LDH/ZnO/CC electrode can be practically applied in flexible supercapacitor. The superb properties of NiCo-LDH/ZnO NF/CC electrode and NiCo-LDH/ZnO NF//AC ASC are attributable to the introduction of ZnO that facilitates the transmission of electrons, and NiCo-LDH nanoflakes grown on ZnO nanoflakes that expand the contacting area between the electrode and electrolyte to expose more redox-active locations, boosting the electrochemical performance of the composite electrode and assembled supercapacitor.

5. CRediT authorship contribution statement

Haotian Xiong: Conceptualization, Investigation, Methodology, Data curation, Writing - original draft. **Lianlian Liu:** Conceptualization, Methodology, Data curation. **Liang Fang:** Resources, Writing - review & editing, Validation, Supervision. **Fang Wu:** Validation, Supervision. **Shufang Zhang:** Software. **Haijun Luo:** Formal analysis. **Cunzhu Tong:** Visualization. **Baoshan Hu:** Writing - review & editing. **Miao Zhou:** Writing - review & editing.

Declaration of Competing Interest

The authors declare that they have no known competing financial interests or personal relationships that could have appeared to influence the work reported in this paper.

Acknowledgements

This work was supported by the Fundamental Research Funds for the Central Universities (2020CDCGJ002, 2019CDXYWL0029, and 2018CDJDWL0011), the Natural Science Foundation of Chongqing (cstc2019jcyj-msxmX0566, cstc2018jcyjAX0450, cstc2018jcyjA2923, and cstc2017jcyjAX0393), the Projects of President Foundation of Chongqing University (2019CDXZWL002), the Opening Project of State Key Laboratory of Luminescence and Applications (SKLA-2020-10), Chongqing Key Laboratory of Micro/Nano Materials Engineering and Technology (KFJJ1301), and the Sharing Fund of Large-scale Equipment of Chongqing University (202003150060 and 202003150078). XRD and SEM were performed by the Analytical and Testing Center of Chongqing University.

References

- [1] S. Chu, A. Majumdar, Opportunities and challenges for a sustainable energy future, *Nature* 488 (2012) 294–303.
- [2] H. Nishide, K. Oyaizu, Materials science - toward flexible batteries, *Science* 319 (2008) 737–738.
- [3] V.L. Pushparaj, M.M. Shajjumon, A. Kumar, S. Murugesan, L. Ci, R. Vajtai, R.J. Linhardt, O. Nalamasu, P.M. Ajayan, Flexible energy storage devices based on nanocomposite paper, *Proc. Natl. Acad. Sci. U.S.A.* 104 (2007) 13574–13577.
- [4] M.Q. Ge, J. Zhang, J. Xu, J.L. Lei, L.J. Li, In-situ fabrication of self-collected Ni(OH)₂ supercapacitor electrode materials by hydrothermal treatment of Ni foam in H₂O₂ solution, *Surf. Technol.* 44 (2015) 47–50.
- [5] Q.N. Zhong, Z.L. Su, X.L. Li, Preparation and supercapacitor performance of a flexible nitrogen-doped graphene film, *Surf. Technol.* 44 (2015) 51–55.
- [6] D.P. Dubal, J.G. Kim, Y. Kim, R. Holze, C.D. Lokhande, W.B. Kim, Supercapacitors based on flexible substrates: an overview, *Energy Technol.* 2 (4) (2014) 325–341.
- [7] D.G. Evans, R.C.T. Slade, Structural aspects of layered double hydroxides, in: X. Duan, D.G. Evans (Eds.), *Layer. Double Hydrox.* 2006, pp. 1–87.
- [8] Y. Lu, B. Jiang, L. Fang, F. Ling, F. Wu, B. Hu, F. Meng, C. Niu, F. Lin, H. Zheng, An investigation of ultrathin nickel-iron layered double hydroxide nanosheets grown on nickel foam for high-performance supercapacitor electrodes, *J. Alloy. Compd.* 714 (2017) 63–70.
- [9] A. Malak-Polaczyk, C. Vix-Guterl, E. Frackowiak, Carbon/layered double hydroxide (LDH) composites for supercapacitor application, *Energy Fuels* 24 (6) (2010) 3346–3351.
- [10] W. Su, F. Wu, L. Fang, J. Hu, L. Liu, T. Guan, X. Long, H. Luo, M. Zhou, NiCo-LDH nanowires@nanosheets core-shell structure grown on carbon fiber cloth for high performance flexible supercapacitor electrode, *J. Alloy. Compd.* 799 (2019) 15–25.
- [11] G. Nagaraju, G.S.R. Raju, Y.H. Ko, J.S. Yu, Hierarchical Ni-Co layered double hydroxide nanosheets entrapped on conductive textile fibers: a cost-effective and flexible electrode for high-performance pseudocapacitors, *Nanoscale* 8 (2016) 812–825.
- [12] J.C. Chen, C.T. Hsu, C.C. Hu, Superior capacitive performances of binary nickel-cobalt hydroxide nanonetwork prepared by cathodic deposition, *J. Power Sour.* 253 (2014) 205–213.
- [13] X. Liu, J. Huang, X. Wei, C. Yuan, T. Liu, D. Cao, J. Yin, G. Wang, Preparation and electrochemical performances of nanostructured Co_xNi_{1-x}(OH)₂ composites for supercapacitors, *J. Power Sour.* 240 (2013) 338–343.
- [14] X. Wang, C. Yan, A. Sumboja, J. Yan, P.S. Lee, Achieving high rate performance in layered hydroxide supercapacitor electrodes, *Adv. Energy Mater.* 4 (2014) 1301240.
- [15] B. Patil, C. Park, H. Ahn, Scalable nanohybrids of graphitic carbon nitride and layered NiCo hydroxide for high supercapacitive performance, *RSC Adv.* 9 (58) (2019) 33643–33652.
- [16] X. Cai, X. Shen, L. Ma, Z. Ji, C. Xu, A. Yuan, Solvothermal synthesis of NiCo-layered double hydroxide nanosheets decorated on RGO sheets for high performance supercapacitor, *Chem. Eng. J.* 268 (2015) 251–259.
- [17] Y.M. Jeong, I. Son, S.H. Baek, Binder-free of NiCo-layered double hydroxides on Ni-coated textile for wearable and flexible supercapacitors, *Appl. Surf. Sci.* 467 (2019) 963–967.
- [18] Y. Cheng, H. Zhang, C.V. Varanasi, J. Liu, Improving the performance of cobalt-nickel hydroxide based self-supporting electrodes for supercapacitors using accumulative approaches, *Energy Environ. Sci.* 6 (2013) 3314–3321.
- [19] H. Niu, D. Zhou, X. Yang, X. Li, Q. Wang, F. Qu, Towards three-dimensional hierarchical ZnO nanofiber@Ni(OH)₂ nanoflake core-shell heterostructures for high-performance asymmetric supercapacitors, *J. Mater. Chem. A* 3 (2015) 18413–18421.
- [20] X. Sun, Q. Li, Y. Lu, Y. Mao, Three-dimensional ZnO@MnO₂ core@shell nanostructures for electrochemical energy storage, *Chem. Commun.* 49 (2013) 4456–4458.
- [21] H. Pang, Y. Ma, G. Li, J. Chen, J. Zhang, H. Zheng, W. Du, Facile synthesis of porous ZnO-NiO composite micropolyhedrons and their application for high power supercapacitor electrode materials, *Dalton Trans.* 41 (2012) 13284–13291.
- [22] D. Cai, H. Huang, D. Wang, B. Liu, L. Wang, Y. Liu, Q. Li, T. Wang, High-performance supercapacitor electrode based on the unique ZnO@Co₃O₄ Core/Shell heterostructures on nickel foam, *ACS Appl. Mater. Interfaces* 6 (2014) 15905–15912.
- [23] I. Shakir, M. Shahid, U.A. Rana, I.M. Al Nashef, R. Hussain, Nickel-cobalt layered double hydroxide anchored zinc oxide nanowires grown on carbon fiber cloth for high-performance flexible pseudocapacitive energy storage devices, *Electrochim. Acta* 129 (2014) 28–32.
- [24] N.T.H. Trang, H. Van Ngoc, N. Lingappan, D.J. Kang, A comparative study of supercapacitive performances of nickel cobalt layered double hydroxides coated on ZnO nanostructured arrays on textile fibre as electrodes for wearable energy storage devices, *Nanoscale* 6 (2014) 2434–2439.
- [25] J. Huang, T. Lei, X. Wei, X. Liu, T. Liu, D. Cao, J. Yin, G. Wang, Effect of Al-doped β-Ni(OH)₂ nanosheets on electrochemical behaviors for high performance supercapacitor application, *J. Power Sour.* 232 (2013) 370–375.
- [26] Y. Lu, B. Jiang, L. Fang, S. Fan, F. Wu, B. Hu, F. Meng, Highly sensitive non-enzymatic glucose sensor based on 3D ultrathin NiFe layered double hydroxide nanosheets, *Electroanalysis* 29 (2017) 1755–1761.
- [27] M. Li, L. Fang, H. Zhou, F. Wu, Y. Lu, H. Luo, Y. Zhang, B. Hu, Three-dimensional porous MXene/NiCo-LDH composite for high performance non-enzymatic glucose sensor, *Appl. Surf. Sci.* 495 (2019) 143554.
- [28] Y.-Y. Liang, S.-J. Bao, H.-L. Li, Nanocrystalline nickel cobalt hydroxides/ultrastable Y zeolite composite for electrochemical capacitors, *J. Solid State Electrochem.* 11 (2007) 571–576.
- [29] T. Guan, L. Fang, Y. Lu, F. Wu, F. Ling, J. Gao, B. Hu, F. Meng, X. Jin, A facile approach to synthesize 3D flower-like hierarchical NiCo layered double hydroxide microspheres and their enhanced adsorption capability, *Coll. Surf. A Physicochem. Eng. Asp.* 529 (2017) 907–915.

- [30] T. Guan, L. Fang, L. Liu, F. Wu, Y. Lu, H. Luo, J. Hu, B. Hu, M. Zhou, Self-supported ultrathin NiCo-LDH nanosheet array/Ag nanowire binder-free composite electrode for high-performance supercapacitor, *J. Alloy. Compd.* 799 (2019) 521–528.
- [31] L. Liu, T. Guan, L. Fang, F. Wu, Y. Lu, H. Luo, X. Song, M. Zhou, B. Hu, D. Wei, Self-supported 3D NiCo-LDH/Gr composite nanosheets array electrode for high-performance supercapacitor, *J. Alloy. Compd.* 763 (2018) 926–934.
- [32] M. Li, K. Ma, J. Cheng, D. Lv, X. Zhang, Nickel-cobalt hydroxide nanoflakes conformal coating on carbon nanotubes as a supercapacitive material with high-rate capability, *J. Power Sour.* 286 (2015) 438–444.
- [33] Y. Guo, X. Hong, Y. Wang, Q. Li, J. Meng, R. Dai, X. Liu, L. He, L. Mai, Multicomponent hierarchical Cu-doped NiCo-LDH/CuO double arrays for ultra-long-life hybrid fiber supercapacitor, *Adv. Funct. Mater.* 29 (2019) 1809004.
- [34] H. Li, F. Musharavati, E. Zalenezhad, X. Chen, K.N. Hui, K.S. Hui, Electrodeposited NiCo layered double hydroxides on titanium carbide as a binder-free electrode for supercapacitors, *Electrochim. Acta* 261 (2018) 178–187.
- [35] X. Gong, J. Cheng, F. Liu, L. Zhang, X. Zhang, Nickel-Cobalt hydroxide microspheres electrodeposited on nickel cobaltite nanowires grown on Ni foam for high-performance pseudocapacitors, *J. Power Sour.* 267 (2014) 610–616.